Facile synthesis, structural and optical characterizations of Bi12ZnO20 sillenite crystals: Application for Cefuroxime removal from wastewater

O. Baaloudj, N. Nasrallah, A.A. Assadi

Facile synthesis, structural and optical characterizations of $Bi_{12}ZnO_{20}$ sillenite crystals: application for Cefuroxime removal from wastewater.

Oussama BAALOUDJ [a]*, Noureddine NASRALLAH [a]*, Aymen Amin ASSADI [b]

[a] Laboratory of Reaction Engineering, Faculty of Mechanical Engineering and Process Engineering, USTHB, BP 32, 16111 Algiers, Algeria.

[b] Univ Rennes – ENSCR-11, Alée de beaulieu – CS 50837 - 35708 Rennes Cedex 7, France.

* Corresponding author E-mail address: obaaloudj@usthb.dz (Oussama Baaloudj).

nas_nour@yahoo.fr (Noureddine Nasrallah).

Abstract

The purpose of this work is to study the structural and optical properties of the bismuth-based zinc sillenite $Bi_{12}ZnO_{20}$ (BZO) in order to characterize a new catalyst that could be used for environmental application. BZO nanoparticles were synthesized by the co-precipitation technique. The obtained catalyst was characterized by different techniques. Starting with X-ray diffraction (XRD), the structure was refined from XRD data using the Rietveld method and then illustrated the structural form of this sillenite for the first time. A space group of I23 with a lattice parameter (a = 10.213815 Å) was found for this crystal. Also, a special surface area (SSA) of 12.31 m^2/g for BZO was determined by the Brunauer-Emmett-Teller (BET) method. Then, the morphology of the nanoparticles was visualized by Scanning Electron Microscope (SEM). The optical proprieties of BZO have been evaluated by UV-VIS diffusion reflectance spectroscopy (DRS), an optical bandgap of 2.8 eV was found. This narrow bandgap allows this sillenite to be a promising and successful photocatalyst for photocatalytic applications. For that, we tested for a hazardous antibiotic from a pharmaceutical industry which is Cefuroxime, this catalyst has shown very interesting activity in degrading this pollutant around 80% in just 4h. This rate is the highest compared to the literature.

Keywords: Sillenite $Bi_{12}ZnO_{20}$, Structural form, Rietveld method, Optical properties.

1. Introduction

Photocatalysis has proved to be a promising solution for the rapid degradation of recalcitrant and non-biodegradable compounds in water, H_2 production through water splitting, and CO_2 reduction [1,2]. It is based on semiconductors (catalysts) that can be activated and excited by a light source such as sunlight and used this energy to remove different types of

pollutants [3]. Based on my previous studies, photocatalysis using semiconductors has successfully removal for both organic and inorganic pollutants in the wastewater [4,5]. So it is important to develop and test new semiconductors with high photocatalytic activity and narrow bandgap.

The rise in the search in recent years for new material categories allowed new studies on structural and optical properties [6,7]. Among these materials, sillenites materials are recent photocatalysts that attract a lot of scientists due to their unique crystal structures, their peculiar electronics, their interesting photochromic, photorefractive, electro-optic, piezoelectric, dielectric properties, promising optical activity [8–10]. They are used in various industrial applications such as image amplification, phase conjugation, real-time and multiwavelength holography, optical memories for data storage, optical communications, signal processing and a variety of photocatalytic applications [11,12]. Sillenite crystals with a general formula $Bi_{12}MO_{20}$ (BMO), is a body-centered cubic crystal structure crystallize in the I 2 3 space group [13,14]. Their overall structure is described in the atom of bismuth surrounded by seven oxygen atoms that share corners with other similar Bi polyhedra and with MO_4 which represents a tetravalent ion or a combination of ions that exist both at the cube center and on the corners in the BMO structure [15–19]. There are a significant number of new sillinetes that are used as photo-catalysts in previous researches, such as $Bi_{12}CoO_{20}$, $Bi_{12}NiO_{19}$, $Bi_{12}TiO_{20}$, $Bi_{12}GeO_{20}$, $Bi_{12}PbO_{19}$ and $Bi_{12}ZnO_{20}$ [8–11,13–17,20,21]. Among those sillenites, the bismuth-based zinc metal sillenite $Bi_{12}ZnO_{20}$ (BZO) has attracted great interest recently due to its narrow bandgap 2.8 eV, its high photoconductivity, facile recycling and stability [22–24]. BZO is a lead-free and environmentally friendly material which makes it very promising for photocatalytic application.

Therefore, we now report in this study the synthesis of $Bi_{12}ZnO_{20}$ sillenite by the co-precipitation method. Firstly, the phase of the crystals was identified by X-ray diffraction (XRD) then the structure and lattice constants of the phase were refined using the Rietveld method. Also, the special surface area (SSA) of BZO was determined by the Brunauer-Emmett-Teller (BET) method. Then, the morphology of the nanoparticles was investigated by Scanning Electron Microscope (SEM). After that, the BZO's optical properties were investigated using UV-VIS diffusion reflectance spectroscopy (DRS) and the obtained bandgap was discussed. Finally, its photocatalytic activity was tested for the degradation of the hazardous antibiotic Cefuroxime.

2. Material and methods

2.1 Chemicals

The products used in the present study were: zinc nitrate hexahydrate [$Zn(NO_3)_2{\cdot}6H_2O$] (98% Biochem), bismuth nitrate pentahydrate [$Bi(NO_3)_3{\cdot}5H_2O$] (98.5% Chem-Lab), ammonia from Biochem and ethanol, nitric acid NaOH, HCl from Sigma Aldrich. Cefuroxime (CFRM) $C_{16}H_{16}N_4O_8S$ was supplied by Parmallience a pharmaceutical company in Algeria. Distilled water was used as a solvent. Without further purification, all chemicals have been used as obtained.

2.2 Preparation of the sillenite $Bi_{12}ZnO_{20}$

The bismuth-based zinc metal $Bi_{12}ZnO_{20}$ (sillenite type) was synthesized by mixing bismuth nitrate [$Bi(NO_3)_3{\cdot}5H_2O$] and zinc nitrate [$Zn(NO_3)_2{\cdot}6H_2O$] in stoichiometric amounts, dissolved with a magnetic stirring in ethanol. After total solubility, the two solutions were mixed and placed on a hot plate at 50 °C for one hour. Over 5% HNO_3 acid was added to the solutions for better solubility. The reaction is carried out according to the following equation:

$$12\,[Bi(NO_3)_3{\cdot}5H_2O] + [Zn(NO_3)_2{\cdot}6H_2O] \rightarrow Bi_{12}ZnO_{20} + 38\,NO_2 + 66\,H_2O + 9\,O_2 \quad (1)$$

Then, to keep the pH between 9 and 10, the NaOH (6 M) solution was thoroughly mixed into the mixture. White precipitation confirmed the formation of BZO spinel immediately. As a result, the precipitate was extracted and washed several times with distilled water before being dried in an autoclave at 120°C for 24 h. An amorphous powder and after that denitrified at 600 ° C for 3 h. Before calcination, the obtained powder was homogenized by grinding in an agate mortar, then it was calcined in an air oven at 800 ° C for 6 h. The calcination step was done to increase the crystallinity. Finally, the end product with a whitish-yellow color was subjected to phase identification step, structural characterization and optical study.

Fig. 1 Process of the preparation of the sillenite $Bi_{12}ZnO_{20}$.

2.3 Characterization

. The X-ray diffraction (XRD) was performed using a Phillips PW 1730, the structural, refinement and crystal measurement was done by Rietveld technique using the MAUD software (ver 2.93). The structure illustration was performed using VESTA (ver 3.4.0). the images of the crystals have been taken by the electron scanning microscope FEI Quanta 650. The UV-visible diffuse reflection (DRS) of the sample was analyzed using Cary 5000 UV-Vis.

2.4 Photocatalytic efficiency study

The photocatalytic efficiency of this material was tested for treating the antibiotic Cefuroxime (CFRM) that is non-biodegradable and has a hazardous effect on the environment. The photocatalytic test was done after the optimization of parameters such as pH and catalyst dosage. Temperature at 25 °C, pH 6, 1 g/L dose and CFRM initial concentration of 5 mg/L were the optimum photocatalytic reaction conditions. Before irradiation, the sample was kept in the dark for 120 minutes to establish the adsorption-desorption equilibrium. A tungsten lamp (200 W) from Osram was utilized as a light irradiation source, and it was situated 10 cm away from the solution's surface. The CFRM concentration was controlled using UV - Visible Spectrophotometer (OPTIZEN, 3220 UV) by measuring the maximum absorbance at the wavelength ($\lambda_{max} = 280\ nm$).

3. Results and discussion

3.1 Characterization of the sillenite $Bi_{12}ZnO_{20}$

3.1.1 Phase identification and structural investigation

To investigate the formation of the sillenite crystals $Bi_{12}ZnO_{20}$, X-ray diffraction (XRD) was used (Fig. 2). All diffraction peaks are narrow and well indexed to the cubic phase of BZO with the JCPDS card number 78–1325, this is in line with the literature [25,26]. The XRD data and an I23 cubic structure were used to conduct Rietveld refinement, experimental findings and theoretical data determined by Maud are shown in Figure 1 as points and red lines respectively. The results showed that the findings calculated by the technique Rietveld are well matched with the experimental X-ray diffraction pattern. The Rietveld refinement results gave identical results compared to other known methods of structural properties [27]. The refined values represented a cubic structure with a space group I23 and a lattice parameter (a = 10.213815 Å). The Rietveld refined parameters such as reliability factors R_b, R_{exp}, R_{wp} and Sig with the cell parameter (a) and atomic position (x,y,z) are presented in Table 1.

Fig. 2 XRD diffractogram with Reitveld refinement *of* the sillenite $Bi_{12}ZnO_{20}$.

Table 1 Rietveld and structural parameters.

The structural representation of the sillenite BZO was illustrated in Fig. 3 by Vesta using the structural parameters in table 1. The atoms' colors for Zn, Bi and O are gray, yellow and red, respectively. As can be seen, the phase is a cubic structure (space group I23). The atoms in

the crystal structure aren't shared occupancy between bismuth and zinc, where the occupancy of each atom is 1.

Fig. 3: the structural representation of the crystal $Bi_{12}ZnO_{20}$.

The crystallite size, X-ray density, and special surface area were calculated from the following equations [28]:

$$D = \frac{K\lambda}{\beta\cos(\theta)} \tag{2}$$

$$\rho = \frac{ZM}{N_A V} \tag{3}$$

$$S = \frac{6 \times 10^3}{D \times \rho} \tag{4}$$

Where D is the regular phase crystallite, K is the Scherener constant, β is the full width at the highest half of the phase, θ is the angle Braggs, N_A is Avogadro's number, M is the Molecular mass of BZO (2893.14 g.mol^{-1}), ρ is the density of X-ray, Z is the count of model units in a cell (Z = 2 for sillenites [29]) and V is the unit cell volume (1065.524205 Å ^{3}) and S is the specific surface area.

The crystallite size was calculated from the highest diffraction peak of the XRD diffractogram and it was found 54.15 nm. The density of X-rays was found to be 9 g/cm^3. The special surface area (SSA) of the particular BZO was estimated by the Brunauer-Emmett-Teller (BET) method in equ. 4 and it was found 12.31 m^2/g.

3.1.2 Morphology investigation

In order to analyze the morphology of the BZO crystals, Scanning Electron Microscopy (SEM) was used. Figure 4 shows a typical SEM image of the sample. It can be observed that the particles are slightly agglomerated due to the ultrafine nature of the sample, leading to the inhomogeneous distribution of crystals with different shapes and a noticeable porosity. The viscosity of the suspension in the synthesis route plays an important role in the development of the porous structure [1,30]. The porous structure becomes compact by increasing the viscosity of the suspension during the synthesis. The co-precipitation method is well known for its great viscosity because it forms precipitation during the synthesis, for that we have significant porosity in our sample.

Fig. 4 SEM images of the crystals $Bi_{12}ZnO_{20}$.

3.1.3 Optical study

The knowledge of the gap is very important to determine the photocatalytic performance of the catalyst. For that, the optical properties of BZO crystals were investigated by UV-vis diffuse reflectance spectroscopy (DRS). The bandgap energy (Eg) is determined by plotting the Tauc plot (Fig. 5), which is the dependence of the absorption coefficient (α) on the photon energy (hν). It is expressed in the following relationship [31]:

$$(\alpha h\nu)^{\frac{1}{n}} = K(h\nu - E_g) \quad (5)$$

α is the absorption coefficient, K a proportionality constant and the exponent n= 2 or 1/2 refers to the nature of the transition. The direct bandgap was estimated by the interception of the linear plot $(\alpha h\nu)^2$ and the hν axis. The band-gap energy (Eg) of BZO crystals was about 2.8 ± 0.1 eV which is narrow than that of TiO_2 and ZnO (3.2 eV) [32,33]. This shows that BZO has a significant absorption level for the UV region from wavelength 200 to 400 nm where the fraction of the light irradiance is converted into electrical and/or chemical energy [34]. This tends to be more effective than the photocatalysts ZnO and TiO_2 and leads in UV irradiation to an increase in the formation of pairs of electron holes. This narrow bandgap allows this sillenite to be a new promising catalyst for photo-catalysis applications and environmental aquatic pollution treatment.

Fig. 5 UV–Vis diffuse reflectance spectrum of the crystals $Bi_{12}ZnO_{20}$.

3.2 Photocatalytic efficiency investigation

In order to test the efficiency of this catalyst for antibiotic removal, the irradiation photolysis effect must be considered. A test without the Catalyst BZO was conducted under UV irradiation to eliminate the effects of the photolysis. Photolysis recorded only a small percentage of CFRM degradation, not even above 2%. It can therefore be argued that the effect of photolysis could be neglected. Following the neglect of photolysis, we conducted the same experiment under similar conditions, albeit a BZO photocatalyst was present. Fig. 6 demonstrated the degradation rate of CFRM in the presence of BZO as a function of time. Where the inset figure shows the associated UV-vis spectra for each point. As can be seen, the rate of CFRM degradation achieved 80 % within only 240 min which is very high compared to our previous study which is the only study that dealt with CFRM degradation [2]. This is owing to the catalyst's gap energy (2.8 eV) which offers a higher light absorption in the UV region from 200 to 600 nm [34]. It is an extremely difficult effort to improve the photocatalytic

performance of semiconductors from the removal of those hazardous pollutants, especially antibiotics which have difficult chemical composition.

Fig. 6 Photocatalytic activity of $Bi_{12}ZnO_{20}$ for Cefuroxime degradation. Inset: Associated UV-vis spectra.

4. Conclusion and outlook

Within the framework of this study, $Bi_{12}ZnO_{20}$ nanoparticles were synthesized by the co-precipitation method. The obtained catalyst was characterized by different techniques. Starting with X-ray diffraction (XRD), the structure was refined from XRD data using the Rietveld method and then illustrated the structural form of this sillenite for the first time. A space group of I23 with a lattice parameter (a = 10.213815 Å) was found for this semiconductor. Also, the special surface area (SSA) of BZO was determined by the Brunauer-Emmett-Teller (BET) method, it was found 12.31 m^2/g. Then, the morphology of the nanoparticles was visualized by Scanning Electron Microscope (SEM). Finally, the optical properties of BZO were determined by UV-VIS diffusion reflectance spectroscopy (DRS), an optical bandgap of 2.8 eV was found. This narrow bandgap allows this sillenite to be a promising and effective catalyst for photocatalytic applications in the environmental field such as the treatment of polluted water. For that we tested for the removal of Cefuroxime from wastewater, it has shown a very interesting photocatalytic performance around 80% in just 240 min. This rate is very high compared to the literature. We conclude with an outlook on future research, we will test this sillenite in the degradation and the reduction of organic and inorganic pollutants, as they are both hazardous contaminants to the environment.

Acknowledgment

This work was financially supported by both the Faculties of Mechanical Engineering and Process Engineering.

Declaration of competing interest

The authors declare that they have no known competing financial interests or personal relationships that could have appeared to influence the work reported in this paper.

References

[1] O. Baaloudj, N. Nasrallah, M. Kebir, L. Khezami, A. Amrane, A.A. Assadi, A comparative study of ceramic nanoparticles synthesized for antibiotic removal: catalysis characterization and photocatalytic performance modeling, Environ. Sci.

Pollut. Res. 28 (2020) 13900–13912. https://doi.org/10.1007/s11356-020-11616-z.

[2] Y. Benrighi, N. Nasrallah, T. Chaabane, V. Sivasankar, A. Darchen, O. Baaloudj, Photocatalytic performances of ZnCr2O4 nanoparticles for cephalosporins removal: Structural, optical and electrochemical properties, Opt. Mater. (Amst). 115 (2021) 111035. https://doi.org/10.1016/j.optmat.2021.111035.

[3] N. Thi Mai Tho, B. The Huy, D.N. Nha Khanh, N. Quoc Thang, N. Thi Phuong Dieu, B. Dai Duong, N. Thi Kim Phuong, Mechanism of Visible-Light Photocatalytic Mineralization of Indigo Carmine Using ZnBi2O4-Bi2S3 Composites, ChemistrySelect. 3 (2018) 9986–9994. https://doi.org/10.1002/slct.201802151.

[4] H. Kenfoud, N. Nasrallah, O. Baaloudj, D. Meziani, T. Chaabane, M. Trari, Photocatalytic reduction of Cr(VI) onto the spinel CaFe2O4 nanoparticles, Optik (Stuttg). 223 (2020) 165610. https://doi.org/10.1016/j.ijleo.2020.165610.

[5] O. Baaloudj, N. Nasrallah, M. Kebir, B. Guedioura, A. Amrane, P. Nguyen-Tri, S. Nanda, A.A. Assadi, Artificial neural network modeling of cefixime photodegradation by synthesized CoBi2O4 nanoparticles, Environ. Sci. Pollut. Res. 28 (2020) 15436–15452. https://doi.org/10.1007/s11356-020-11716-w.

[6] O.G. Oliveira, A.J. Mincache, G.S. Dias, I.A. Santos, R. Guo, A.S. Bhalla, L.F. Cótica, Study of the crystal and electronic structures of (Bi1−xNdx)FeO3 compositions using Rietveld refinements and the maximum entropy method, Ferroelectrics. 545 (2019) 167–174. https://doi.org/10.1080/00150193.2019.1621702.

[7] W. Bin Im, K. Page, S.P. Denbaars, R. Seshadri, Probing local structure in the yellow phosphor LaSr2AlO 5:Ce3+, by the maximum entropy method and pair distribution function analysis, J. Mater. Chem. 19 (2009) 8761–8766. https://doi.org/10.1039/b912793c.

[8] X. Wu, M. Li, J. Li, G. Zhang, S. Yin, A sillenite-type Bi12MnO20 photocatalyst: UV, visible and infrared lights responsive photocatalytic properties induced by the hybridization of Mn 3d and O 2p orbitals, Appl. Catal. B Environ. 219 (2017) 132–141. https://doi.org/10.1016/j.apcatb.2017.07.025.

[9] X. Lin, F. Huang, W. Wang, Y. Xia, Y. Wang, M. Liu, J. Shi, Photocatalytic activity of a sillenite-type material Bi25GaO39, Catal. Commun. 9 (2008) 572–576. https://doi.org/10.1016/j.catcom.2007.02.004.

[10] H. Zhang, M. Lü, S. Liu, Z. Xiu, G. Zhou, Y. Zhou, Z. Qiu, A. Zhang, Q. Ma, Preparation and photocatalytic properties of sillenite Bi12TiO20 films, Surf. Coatings Technol. 202 (2008) 4930–4934. https://doi.org/10.1016/j.surfcoat.2008.04.081.

[11] D. Hou, X. Hu, Y. Wen, B. Shan, P. Hu, X. Xiong, Y. Qiao, Y. Huang, Electrospun sillenite Bi12MO20 (M = Ti, Ge, Si) nanofibers: General synthesis, band structure, and photocatalytic activity, Phys. Chem. Chem. Phys. 15 (2013) 20698–20705. https://doi.org/10.1039/c3cp53945h.

[12] H. Kenfoud, N. Nasrallah, D. Meziani, M. Trari, Photoelectrochemical study of the spinel CaFe2O4 nanostructure : application to Basic Blue 41 oxidation under solar light, J. Solid State Electrochem. 1–9 (2021). https://doi.org/10.1007/s10008-021-04952-8.

[13] W.F. Yao, H. Wang, X.H. Xu, J.T. Zhou, X.N. Yang, Y. Zhang, S.X. Shang, M. Wang, Sillenites materials as novel photocatalysts for methyl orange decomposition, Chem. Phys. Lett. 377 (2003) 501–506. https://doi.org/10.1016/S0009-2614(03)01209-0.

[14] M. Isik, N. Sarigul, N.M. Gasanly, Thermoluminescence characteristics of Bi12SiO20 single crystals, J. Lumin. 224 (2020) 117280. https://doi.org/10.1016/j.jlumin.2020.117280.

[15] W.F. Yao, X.H. Xu, J.T. Zhou, X.N. Yang, Y. Zhang, S.X. Shang, H. Wang, B.B. Huang, Photocatalytic property of sillenite Bi24AlO39 crystals, J. Mol. Catal. A Chem. 212 (2004) 323–328. https://doi.org/10.1016/j.molcata.2003.11.012.

[16] M. Valant, D. Suvorov, Processing and Dielectric Properties of Sillenite Compounds Bi12MO20-δ (M: Si, Ge, Ti, Pb, Mn, B1/2P1/2)., ChemInform. 33 (2010) no-no. https://doi.org/10.1002/chin.200210013.

[17] P. Zhoua, F. Xiaoa, L. Jia, Bi12NiO19 micro-sheets grown on graphene oxide: Temperature-dependent facile synthesis and excellent electrochemical behavior for supercapacitor electrode, J. Electroanal. Chem. 884 (2021). https://doi.org/10.1016/j.jelechem.2021.115075.

[18] L.Z. Pei, T. Wei, N. Lin, H. Zhang, Synthesis of bismuth nickelate nanorods and electrochemical detection of tartaric acid using nanorods modified electrode, J. Alloys Compd. 663 (2016) 677–685. https://doi.org/10.1016/j.jallcom.2015.12.177.

[19] M. Rajamoorthy, D. Geetha, A. Sathiya Priya, Synthesis of Cobalt-Doped Bi12NiO19: Structural, Morphological, Dielectric and Magnetic Properties, Arab. J. Sci. Eng. 46 (2021) 737–744. https://doi.org/10.1007/s13369-020-04889-6.

[20] H. Kenfoud, O. Baaloudj, N. Nasrallah, R. Bagtache, Structural and electrochemical characterizations of Bi12CoO20 sillenite crystals : degradation and reduction of organic and inorganic pollutants, J. Mater. Sci. Mater. Electron. (2021). https://doi.org/10.1007/s10854-021-06194-w.

[21] Y. Huang, X. Zhang, G. Zhu, Y. Gao, Q. Cheng, X. Cheng, Synthesis of silver phosphate/sillenite bismuth ferrite/graphene oxide nanocomposite and its enhanced visible light photocatalytic mechanism, Sep. Purif. Technol. 215 (2019) 490–499. https://doi.org/10.1016/j.seppur.2019.01.024.

[22] X.L. Wang, Y. Xiao, Z.J. Lv, H. Yu, Y. Yang, X.T. Dong, A novel 2D nanosheets self-assembly camellia-like ordered mesoporous Bi12ZnO20 catalyst with excellent photocatalytic property, J. Alloys Compd. 835 (2020) 155409. https://doi.org/10.1016/j.jallcom.2020.155409.

[23] H. Sekhar, D. Narayana Rao, Preparation, structural and linear optical properties of zinc sillenite (Bi12.66Zn0.33O19.33) nanocrystals, J. Mater. Sci. Mater. Electron. 24 (2013) 1569–1574. https://doi.org/10.1007/s10854-012-0977-1.

[24] J. Tang, J. Ye, Photocatalytic and photophysical properties of visible-light-driven photocatalyst ZnBi12O20, Chem. Phys. Lett. 410 (2005) 104–107. https://doi.org/10.1016/j.cplett.2005.05.051.

[25] A. Muthukrishnaraj, A. Arun, S.S. Kalaivani, T. Maiyalagan, A. Manikandan, N. Balasubramanian, Solvothermal synthesis and characterizations of graphene-ZnBi12O20 nanocomposites for visible-light driven photocatalytic applications, Ceram. Int. 46 (2020) 18534–18543. https://doi.org/10.1016/j.ceramint.2020.04.159.

[26] L. Zhang, X. Zhang, Y.Q. Huang, C.L. Pan, J.S. Hu, C.M. Hou, Novel Bi12ZnO20-Bi2WO6 heterostructures: Facile synthesis and excellent visible-light-driven photocatalytic activities, RSC Adv. 5 (2015) 30239–30247. https://doi.org/10.1039/c5ra01327e.

[27] W.A. Dollase, H.S.C. O'Neill, The spinels CuCr2O4 and CuRh2O4, Acta Crystallogr. Sect. C Cryst. Struct. Commun. 53 (1997) 657–659.

https://doi.org/10.1107/S0108270197000486.

[28] P. Karuppasamy, M. Senthil Pandian, P. Ramasamy, S. Verma, Crystal growth, structural, optical, thermal, mechanical, laser damage threshold and electrical properties of triphenylphosphine oxide 4-nitrophenol (TP4N) single crystals for nonlinear optical applications, Opt. Mater. (Amst). 79 (2018) 152–171. https://doi.org/10.1016/j.optmat.2018.03.041.

[29] T. Growth, The Growth and Melting Morphology of BlaSiO20 Crystals, Ceram. Int. 19 (1993) 211–214.

[30] S. Tripathy, D.S. Saini, D. Bhattacharya, Synthesis and fabrication of MgAl 2 O 4 ceramic foam via a simple, low-cost and eco-friendly method, J. Asian Ceram. Soc. 4 (2016) 149–154. https://doi.org/10.1016/j.jascer.2016.01.008.

[31] P. Makuła, M. Pacia, W. Macyk, How To Correctly Determine the Band Gap Energy of Modified Semiconductor Photocatalysts Based on UV-Vis Spectra, J. Phys. Chem. Lett. 9 (2018) 6814–6817. https://doi.org/10.1021/acs.jpclett.8b02892.

[32] N. Serpone, Is the band gap of pristine TiO2 narrowed by anion- and cation-doping of titanium dioxide in second-generation photocatalysts?, J. Phys. Chem. B. 110 (2006) 24287–24293. https://doi.org/10.1021/jp065659r.

[33] M. Ahmad, W. Rehman, M.M. Khan, M.T. Qureshi, A. Gul, S. Haq, R. Ullah, A. Rab, F. Menaa, Phytogenic fabrication of ZnO and gold decorated ZnO nanoparticles for photocatalytic degradation of Rhodamine B, J. Environ. Chem. Eng. 9 (2021) 104725. https://doi.org/10.1016/j.jece.2020.104725.

[34] O. Baaloudj, A.A. Assadi, M. Azizi, H. Kenfoud, M. Trari, A. Amrane, A.A. Assadi, N. Nasrallah, Synthesis and Characterization of ZnBi2O4 Nanoparticles : Photocatalytic Performance for Antibiotic Removal under Different Light Sources, Appl. Sci. 11 (2021) 3975. https://doi.org/10.3390/app 11093975.

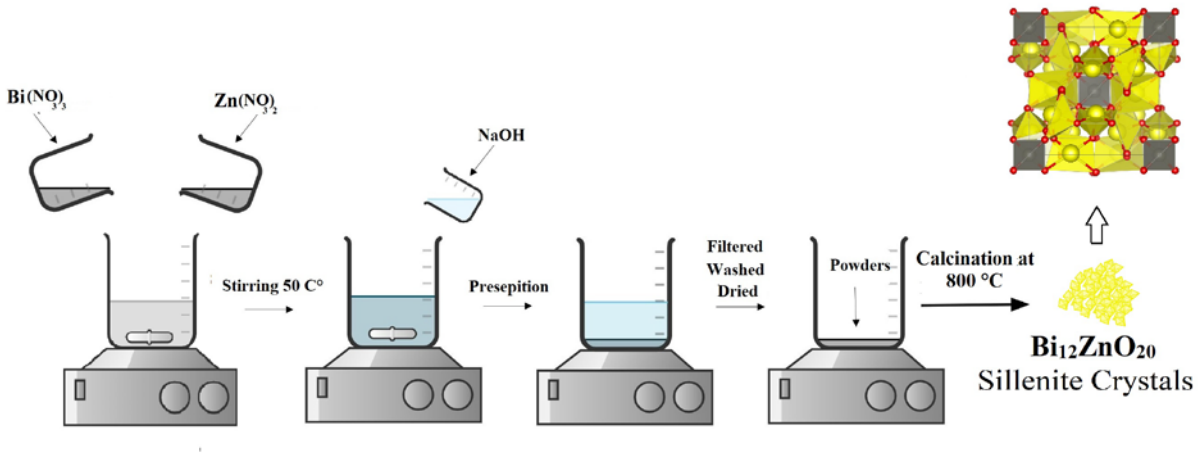

Fig. 1 Process of the preparation of the sillenite $Bi_{12}ZnO_{20}$.

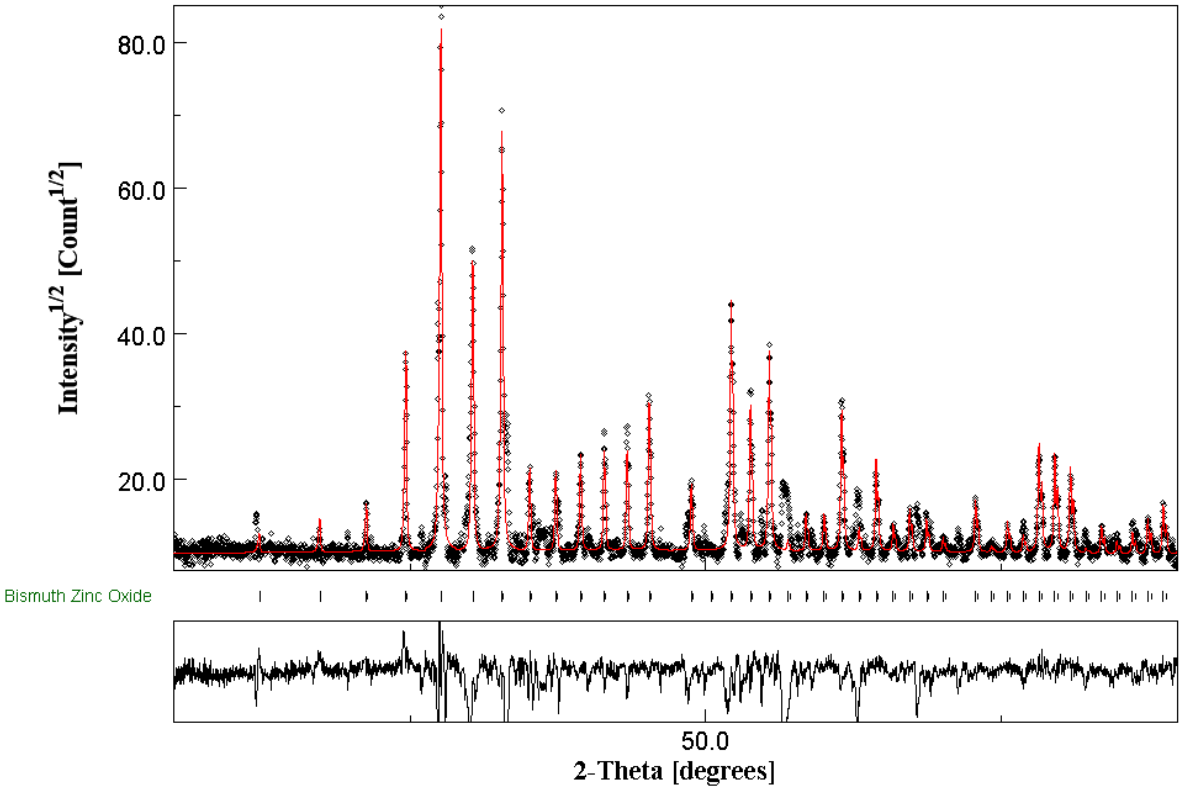

Fig. 2 XRD diffractogram with Reitveld refinement of the sillenite $Bi_{12}ZnO_{20}$.

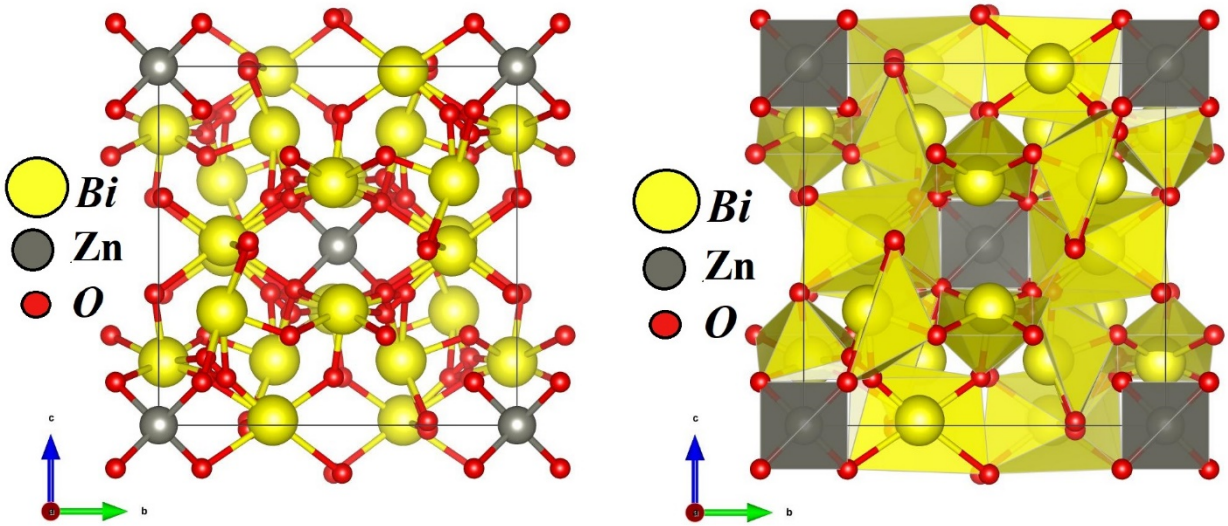

Fig. 3: The structural representation of the crystal $Bi_{12}ZnO_{20}$.

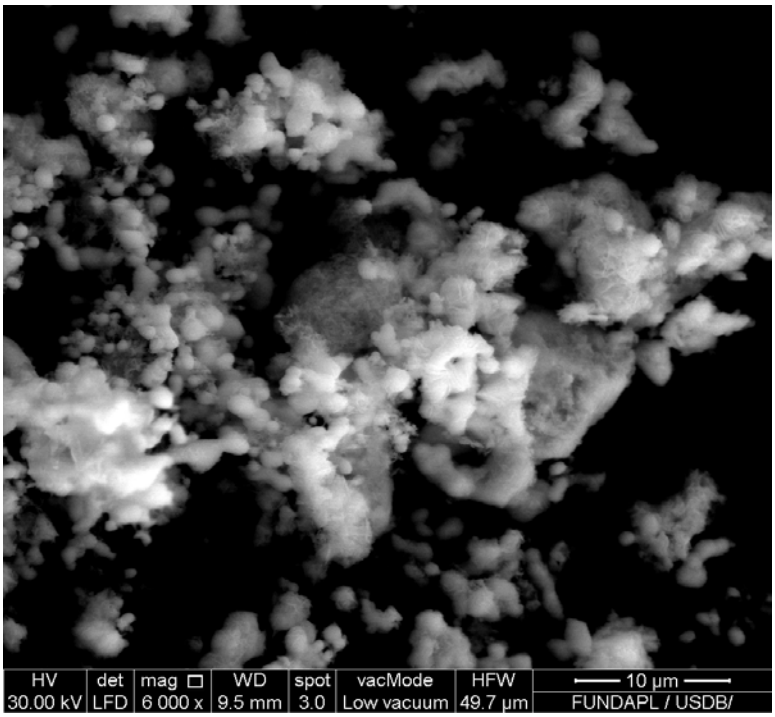

Fig. 4 SEM images of the crystals $Bi_{12}ZnO_{20}$.

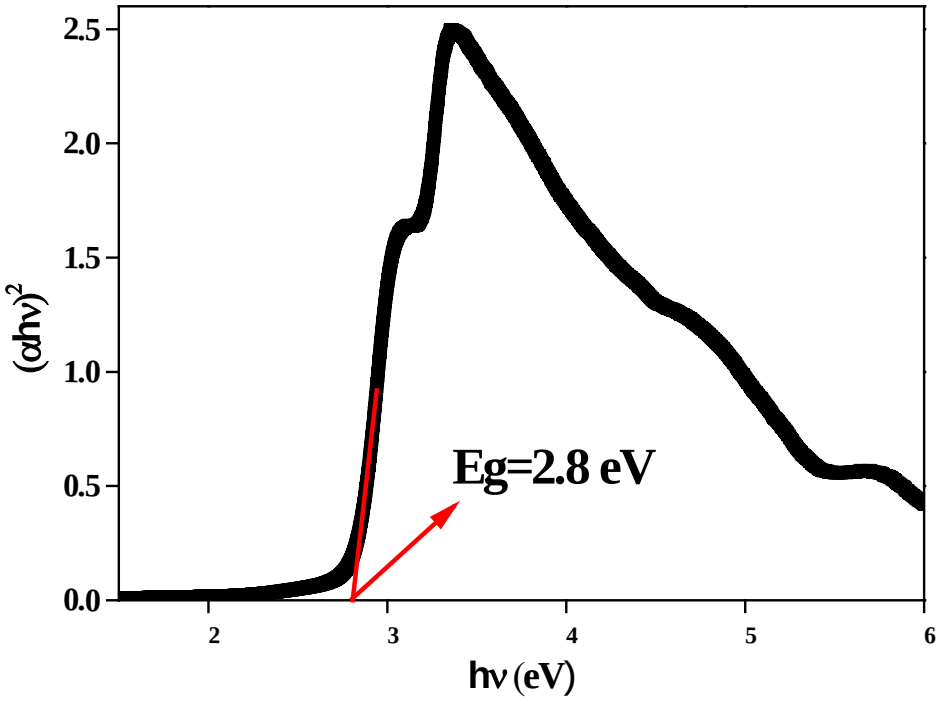

Fig. 5 UV–Vis diffuse reflectance spectrum of the crystals $Bi_{12}ZnO_{20}$.

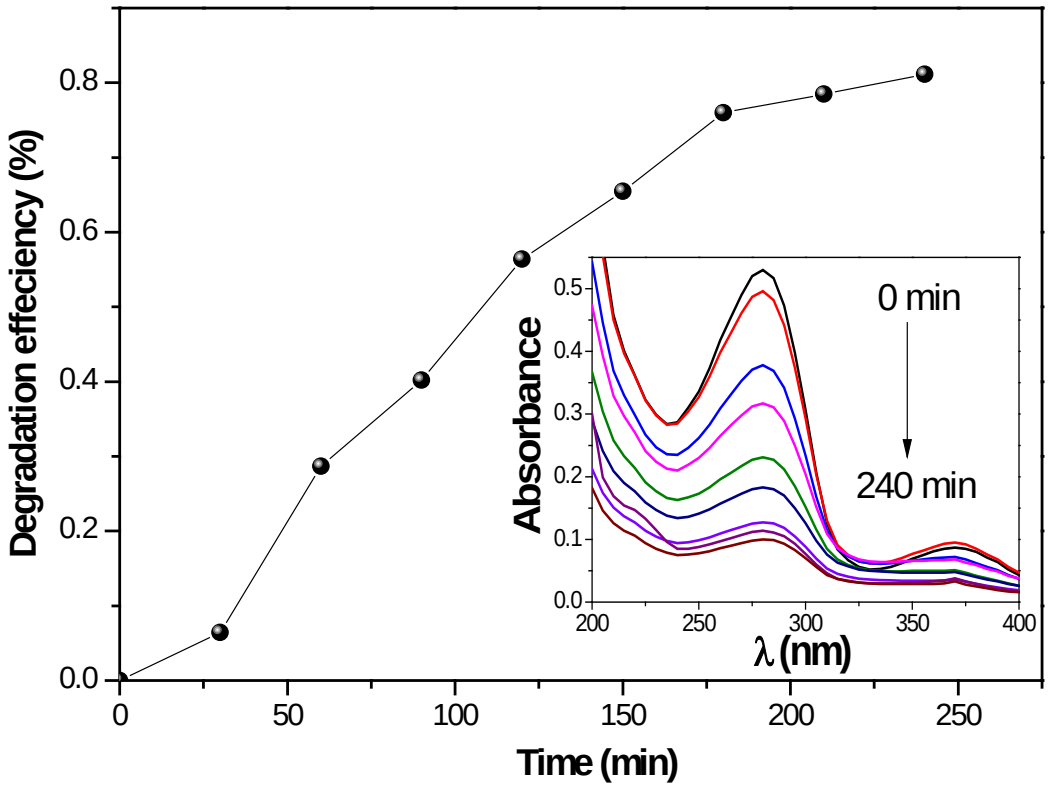

Fig. 6 Photocatalytic activity of $Bi_{12}ZnO_{20}$ for Cefuroxime degradation. Inset: Associated UV-vis spectra.